INFECTION AND IMMUNITY, Oct. 2007, p. 4754–4761 Vol. 75, No. 10
0019-9567/07/$08.00+0 doi:10.1128/IAI.00575-07

Noncapsulated Toxinogenic *Bacillus anthracis* Presents a Specific Growth and Dissemination Pattern in Naive and Protective Antigen-Immune Mice[▽]

Ian J. Glomski, Jean-Philippe Corre, Michèle Mock, and Pierre L. Goossens*

Institut Pasteur, Unité des Toxines et Pathogénie Bactérienne, Paris F-75015, France, and CNRS, URA 2172, Paris F-75015, France

Received 20 April 2007/Returned for modification 10 May 2007/Accepted 9 July 2007

Bacillus anthracis **is a spore-forming bacterium that causes anthrax. *B. anthracis* has three major virulence factors, namely, lethal toxin, edema toxin, and a poly-γ-D-glutamic acid capsule. The toxins modulate host immune responses, and the capsule inhibits phagocytosis. With the goal of increasing safety, decreasing security concerns, and taking advantage of mammalian genetic tools and reagents, mouse models of *B. anthracis* infection have been developed using attenuated bacteria that produce toxins but no capsule. While these models have been useful in studying both toxinogenic infections and antitoxin vaccine efficacy, we questioned whether eliminating the capsule changed bacterial growth and dissemination characteristics. Thus, the progression of infection by toxinogenic noncapsulated *B. anthracis* was analyzed and compared to that by previously reported nontoxinogenic capsulated bacteria, using in vivo bioluminescence imaging. The influence of immunization with the toxin component protective antigen (PA) on the development of infection was also examined. The toxinogenic noncapsulated bacteria were initially confined to the cutaneous site of infection. Bacteria then progressed to the draining lymph nodes and, finally, late in the infection, to the lungs, kidneys, and frequently the gastrointestinal tract. There was minimal colonization of the spleen. PA immunization reduced bacterial growth from the outset and limited infection to the site of inoculation. These in vivo observations show that dissemination by toxinogenic noncapsulated strains differs markedly from that by nontoxinogenic capsulated strains. Additionally, PA immunization counters bacterial growth and dissemination in vivo from the onset of infection.**

Bacillus anthracis is a spore-forming gram-positive bacterium that causes the disease anthrax. Dormant spores are the infectious form of *B. anthracis* (27). The following three distinct forms of anthrax occur: cutaneous, inhalational, and gastrointestinal anthrax (3, 16, 27). Cutaneous anthrax is the most common form in humans and results in a mortality rate of 20% without antibiotic treatment (34). Virulent natural isolates produce two toxins, lethal toxin (LT) and edema toxin (ET) (12, 27), and a poly-γ-D-glutamic acid capsule covalently linked to bacterial cell wall peptidoglycan (7, 25). LT and ET consist of the receptor-binding protective antigen (PA) bound to lethal factor and edema factor, respectively (8). Working in concert, these toxins modulate the host's immune response to promote bacterial survival and can cause cellular death (10, 13, 26, 37). The capsule inhibits phagocytosis, is a nonimmunogenic surface, and is vital for full virulence (7, 9, 25, 33).

The currently approved cell-free human vaccine in the United States, anthrax vaccine absorbed (AVA), predominantly targets PA (23). Although AVA clearly induces the production of anti-PA antibodies (29), the mechanisms by which AVA mediates protection remain uncertain. Studies show that anti-PA antibodies can directly neutralize toxins (29), which eliminates their deleterious effects on the host. Other studies also suggest that anti-PA antibodies bind to the surfaces of spores, leading to both opsonization and greater destruction by phagocytes (40) as well as to inhibition of germination (41). Despite there observations, how toxin neutralization and/or binding of antibodies to spores changes the kinetics of bacterial growth and dissemination remains poorly characterized.

With the goal of increasing safety, decreasing security concerns, and gaining access to powerful mammalian genetic tools and reagents, mouse models of *B. anthracis* infection have been developed using noncapsulated bacteria and mouse strains that are unusually sensitive to infection (19, 43, 44). These models reflect some of the characteristics of wild-type *B. anthracis* infection (19). The most frequently used toxinogenic noncapsulated strain of *B. anthracis* is the Sterne vaccine strain, and the most commonly used sensitive mouse strain is A/J, although DBA/2 mice are also considered sensitive (44). Mouse sensitivity to infection with spores from toxinogenic noncapsulated bacteria has been correlated with the absence of complement component C5 function (43). These complement-deficient mouse models have been useful in both addressing basic questions of toxin-based pathogenesis and the analysis of vaccines, primarily PA-based antitoxin vaccines, that protect against toxinogenic *B. anthracis* infections (42). However, elimination of toxin production while maintaining capsule synthesis does not affect *B. anthracis* virulence in the mouse model of infection (6, 45), despite the fact that the toxins are active at the cellular level (38). This brings into question the relevance of toxins in mouse infections with fully virulent toxinogenic capsulated bacteria.

To date, complement-deficient mouse models of infection have relied on determinations of CFU and mouse survival as

* Corresponding author. Mailing address: Unité des Toxines et Pathogénie Bactérienne, Institut Pasteur, 28 rue du Dr. Roux, 75724 Paris Cedex 15, France. Phone: 33 (0)1 45 68 82 49. Fax: 33 (0)1 45 68 89 54. E-mail: pierre.goossens@pasteur.fr.

▽ Published ahead of print on 16 July 2007.

their primary methods of analysis. These methods lack dynamic analysis of the entire mouse from the initiation of infection to death and therefore provide an incomplete picture of the infectious process. Recently, we described the successful use of bioluminescent nontoxinogenic capsulated *B. anthracis* in murine models of cutaneous, inhalational, and gastrointestinal infections (16). This bioluminescent bacterium can be monitored within the mouse in real time by a technology called in vivo bioluminescence imaging (BLI) (11, 18). Results from this study identified new portals of entry into the host and showed that metabolically active *B. anthracis* is readily detectable and that bioluminescence intensity correlates with CFU (16).

We thus sought to determine the differences in infection dynamics between toxinogenic noncapsulated (referred to hereafter as Tox^+) and previously reported nontoxinogenic capsulated (referred to hereafter as Cap^+) *B. anthracis* strains. Additionally, we wished to determine how PA immunization affects bacterial growth and dissemination in vivo. To achieve this goal, a bioluminescent Tox^+ *B. anthracis* strain was constructed, and infections were analyzed with BLI technology in real time. We found that in contrast to infections with Cap^+ strains, (i) Tox^+ growth is confined to the site of inoculation for a long time, (ii) a minimal number of Tox^+ bacteria are found in the spleen throughout infection, and (iii) the Tox^+ strain infects the kidneys and, frequently, the gastrointestinal tract. Furthermore, PA immunization allows sensitive strains of mice to confine Tox^+ bacteria to the initial site of cutaneous infection without completely eliminating spore germination.

MATERIALS AND METHODS

Bacterial strains, growth conditions, and reagents. Infections were performed with a bioluminescent derivative of the previously described *B. anthracis* strain 9602R (36). 9602R is a derivative of the highly virulent natural human isolate 9602 (5) but has been cured of plasmid pX02 (36) and therefore does not produce a capsule but maintains toxin production, i.e., it is a phenotypic equivalent of the Sterne strain. Bacteria were grown on brain heart infusion (BHI) agar (Difco) unless otherwise noted. Spores were produced and then purified on Radioselectan (Renografin 76%; Schering), using previously described methods, and were stored in sterile deionized water (35). Luminescent 9602R and Sterne (7702) (36) bacteria were constructed as previously described (16). Briefly, *luxABCDE* was inserted into the conjugative shuttle vector pAT113 (35) under the control of the *pagA* promoter, which is highly expressed under in vivo conditions. This vector was then introduced into 9602R by heterogramic conjugation, using previously described methods and the conjugative *Escherichia coli* strain HB101(pRK212.1) (35), and selected on BHI agar containing 5 μg/ml erythromycin, yielding strain 9602Rlux (BIG17).

Image acquisition and analysis. Images were acquired using an IVIS 100 system (Xenogen Corp., Alameda, CA) according to instructions from the manufacturer. Analysis and acquisition were performed using Living Image 2.5 software (Xenogen Corp.). Unless otherwise noted, mice were anesthetized using a constant flow of 2.5% isoflurane mixed with oxygen, using an XGI-8 anesthesia machine (Xenogen Corp.), which allows control of the intensity and duration of anesthesia. Images were acquired with a binning number of 16. Luminescent signals from the exterior of mice were acquired for 1 min, whereas the luminescence of internal organs during dissection was integrated for 10 s. All other photographic parameters were held constant. Quantifying the photons per s emitted by each organ was performed by defining regions of interest corresponding to the organ of interest while subtracting the background, as defined for a noninfected animal in the same photograph.

Infections and immunization of mice. Six- to 10-week-old A/J (Harlan Labs, England), DBA/2J, and BALB/cJ (Charles River Labs, L'Arbresle, France) mice were maintained under specific-pathogen-free conditions at the Pasteur Institute in compliance with European animal welfare regulations. Cutaneous infections were performed under light isoflurane anesthesia by injecting 10 μl of spore suspension in phosphate-buffered saline into the ear with a 0.5-ml insulin syringe (Becton Dickinson, NJ) (4, 16). For CFU determination, organs were removed, placed immediately in ice-cold saline solution, and then homogenized in a chilled glass tube, and dilutions were plated on BHI plates. Lymph node locations and nomenclature were based on previously defined standards (39).

Mice were immunized with PA as previously described (6). In brief, 10 μg of recombinant PA (a kind gift from Les Baillie (Welsh School of Pharmacy, Cardiff University, Cardiff, Wales, United Kingdom) with 0.3% aluminum hydroxide gel (Eurobio, Les Ulis, France) or adjuvant only was injected two times subcutaneously on days 0 and 14. Mice were then infected cutaneously in the ear, as described above, on day 35.

Software and statistical analysis. Standard deviations of CFU, represented by error bars, and Student's unpaired *t* test results, used to compare the luminescent ears of mice with and without PA immunization, were calculated using GraphPad Prism 4. Image analysis was performed with Living Image 2.5 software.

RESULTS

Biosafety level 2 Tox^+ strains of *B. anthracis*, such as the Sterne strain, have been used to model anthrax in the mouse (19, 43, 44), but the capsule is a major virulence factor that contributes to virulence in all models of infection. We thus questioned whether the establishment and dissemination of Tox^+ strains differed markedly from those of previously described capsulated strains (9, 16). A bioluminescent Tox^+ strain (9602Rlux) was constructed and analyzed using in vivo BLI (11, 16, 18). 9602Rlux spores injected cutaneously into the ears of A/J mice gave rise to measurable bioluminescence at the site of injection that disseminated to deeper tissues and ultimately killed the mice (Fig. 1A). Luminescence was detectable 8 h after injection (Fig. 1B) and continued to intensify in the ear until death. At approximately 48 h postinfection, light became detectable in the superficial parotid lymph node (39), draining the ear (Fig. 1A and C). After an increase of luminescence in the ear and lymph node, luminescence spread to the lungs and, unexpectedly, the kidneys, and in 13 of 36 mice (36%) it also spread to the intestines and/or the pyloric region of the stomach as defined foci (Fig. 1C). No luminescence and few CFU were observed in the spleen (Fig. 1C and D), in contrast to observations of infections with luminescent Cap^+ bacteria (16). Dissection late in the infection revealed that both the jejunum and ileum were transparent and distended with a watery liquid (Fig. 1C). By 48 h, edema was observed adjacent to the ear, and by 72 h, it encompassed most of the head and shoulder (data not shown). Similar results were obtained using a luminescent Sterne strain (data not shown).

A comparable, though slower, progression of infection was observed with another sensitive mouse strain (44), DBA/2, where luminescence was confined to the ear for the first 113 h, followed by dissemination to the superficial parotid lymph node at 116 h and then to the lungs, kidneys, and defined foci in the intestines and/or stomach (Fig. 2A to C). A similar percentage of DBA/2 mice developed luminescence in the abdomen (10 of 29 mice [34%]) compared to A/J mice. It should be noted that the dark coloration of DBA/2 mice reduces the sensitivity of bacterial detection since their pigmentation absorbs a greater proportion of emitted light. Similar to the case with A/J mice, edema of the ear, shoulder, and head was evident in DBA/2 mice (data not shown). In contrast, when resistant BALB/c mice (44) were infected, maximal luminescence at the site of injection was observed at 48 h, after which luminescence decreased and was eliminated by 144 h postinfection. Doses of 9602Rlux spores as high as 2.4×10^7 were not

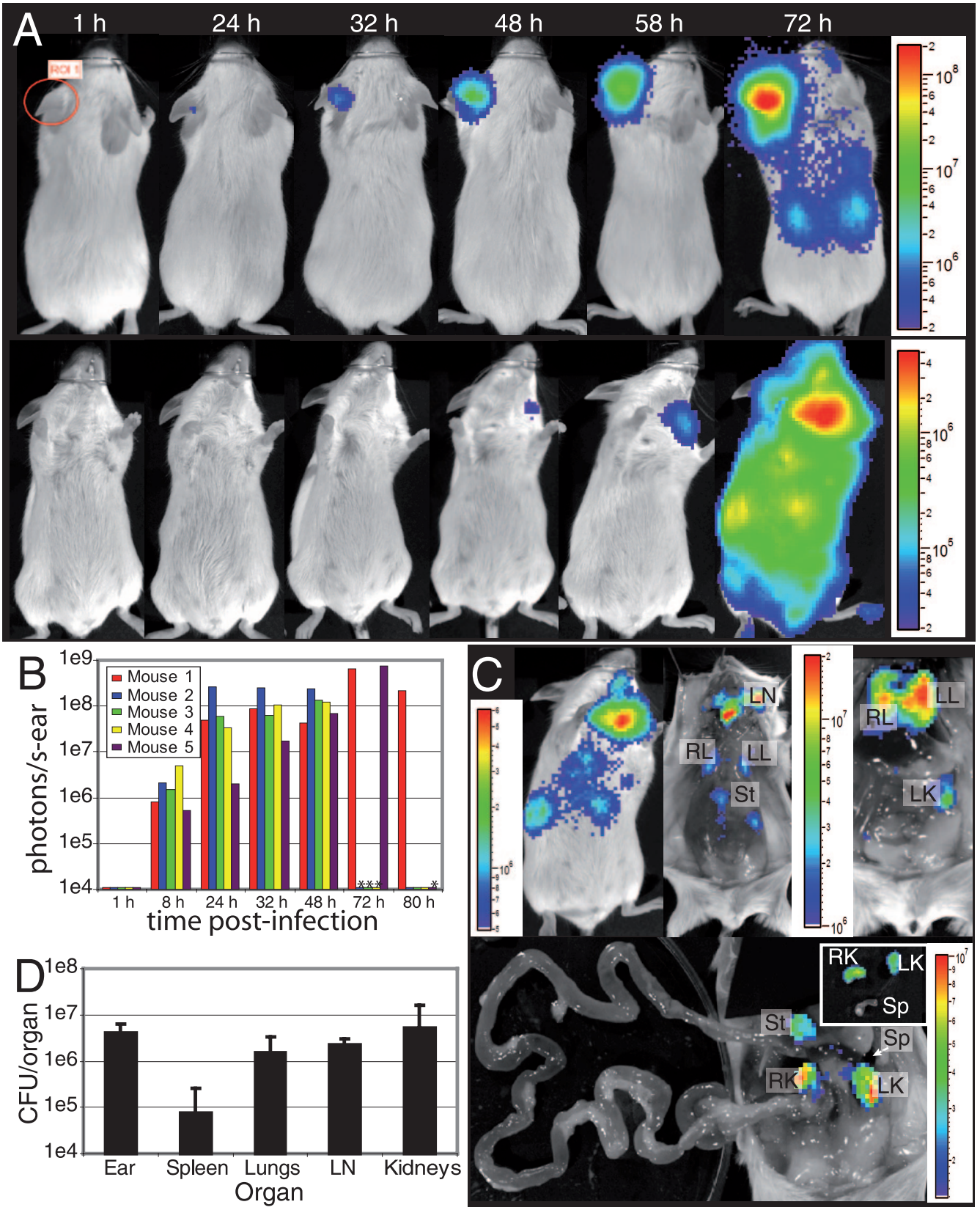

FIG. 1. Dissemination of Tox$^+$ *B. anthracis* organisms in A/J mice. (A) 9602Rlux spores (1×10^4) were injected into the ears of A/J mice and then analyzed for bioluminescence at the indicated times. Images in this figure and the following figures depict photographs overlaid with false-color representations of luminescence intensity, measured in photons/s-cm^2-sr and indicated on the scales, where red is most intense and blue is least intense. (Top row) Dorsal views of a single mouse at the indicated times. (Bottom row) Ventral views of the same mouse, with the infected

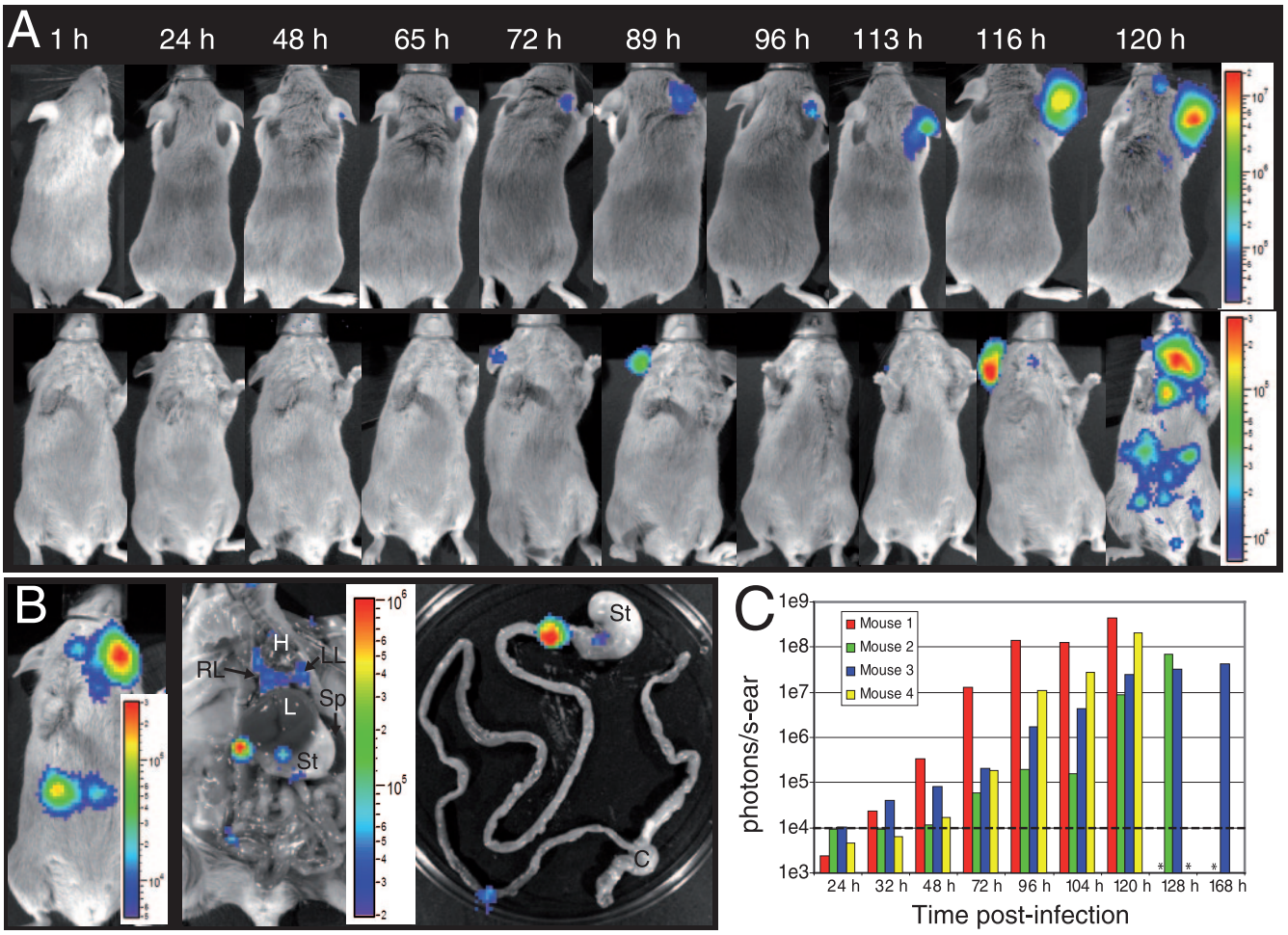

FIG. 2. Dissemination of Tox+ *B. anthracis* organisms in DBA/2 mice. (A) 9602Rlux spores (1×10^5) were injected into the ears of DBA/2 mice and then analyzed as described in the legend to Fig. 1. (Top row) Dorsal views of a single mouse at the indicated times. (Bottom row) Ventral views of the same mouse. Note that the luminescent ear visible in the dorsal images was hidden by the head at 96, 113, and 120 h. The image series is representative of 16 infected mice. (B) A mouse infected for 116 h was dissected to determine which organs were the sources of bioluminescence. (Left) Exterior of the infected mouse. (Center) Opened thorax and peritoneum, with the highly luminescent neck lymph nodes hidden by the sternum. (Right) Ex vivo analysis of the gastrointestinal tract. Abbreviations: H, heart; RL, right lung; LL, left lung; L, liver; St, stomach; Sp, spleen; C, cecum. (C) The luminescence of the ears of mice was quantified at the indicated times by defining specific ROI encompassing the ear. Four individual mice are represented in the graph as differently colored bars. The dotted line represents the detection limit of luminescence. *, the corresponding mouse died.

lethal to BALB/c mice. These BALB/c mice lacked obvious edema yet had scars in the infected dermis after the bacteria had been cleared (Fig. 3A and B).

PA-based vaccines protect from toxinogenic *B. anthracis* infection (27, 42), but where and when adaptive immunity exerts its protective function in vivo remain poorly defined. PA-immunized A/J mice or control mice treated with adjuvant only were infected cutaneously with 9602Rlux spores (Fig. 4A to C). Within 8 h, luminescence in the PA-immunized mice was detected at the site of injection in the ear, remained at a plateau until 32 h, and then diminished in intensity until it was no longer detectable (Fig. 4B and C). Luminescence was not detected beyond the ear in PA-immunized mice. There was significantly more luminescence initiated by 8 h at the site of

ear hidden to allow greater sensitivity in detecting bacteria in the draining lymph node. A single representative region of interest (ROI) for the ear is depicted as a red circle at 1 h. This image series is representative of 30 infected mice. (B) The luminescence of the ears of mice was quantified at the indicated times by defining specific ROI encompassing the ear, as depicted in panel A. Five mice are represented individually in the graph as differently colored bars. The limit of detection was 1×10^4 photons/s-ear. *, the corresponding mouse died. (C) A mouse infected for 72 h was dissected to determine which organs were the sources of bioluminescence. (Top left) Exterior of the infected mouse. (Top center) Dissection with displacement of the skin. (Top right) Open thorax and peritoneum. (Bottom) Uncoiled gastrointestinal tract with the strong luminescence from the neck lymph nodes and thorax blocked. (Inset) Ex vivo analysis of the kidneys and spleen. Abbreviations: LN, lymph nodes; RL, right lung; LL, left lung; St, stomach; LK, left kidney; RK, right kidney; Sp = spleen. (D) CFU were determined for the indicated organs (means plus standard deviations; $n = 4$).

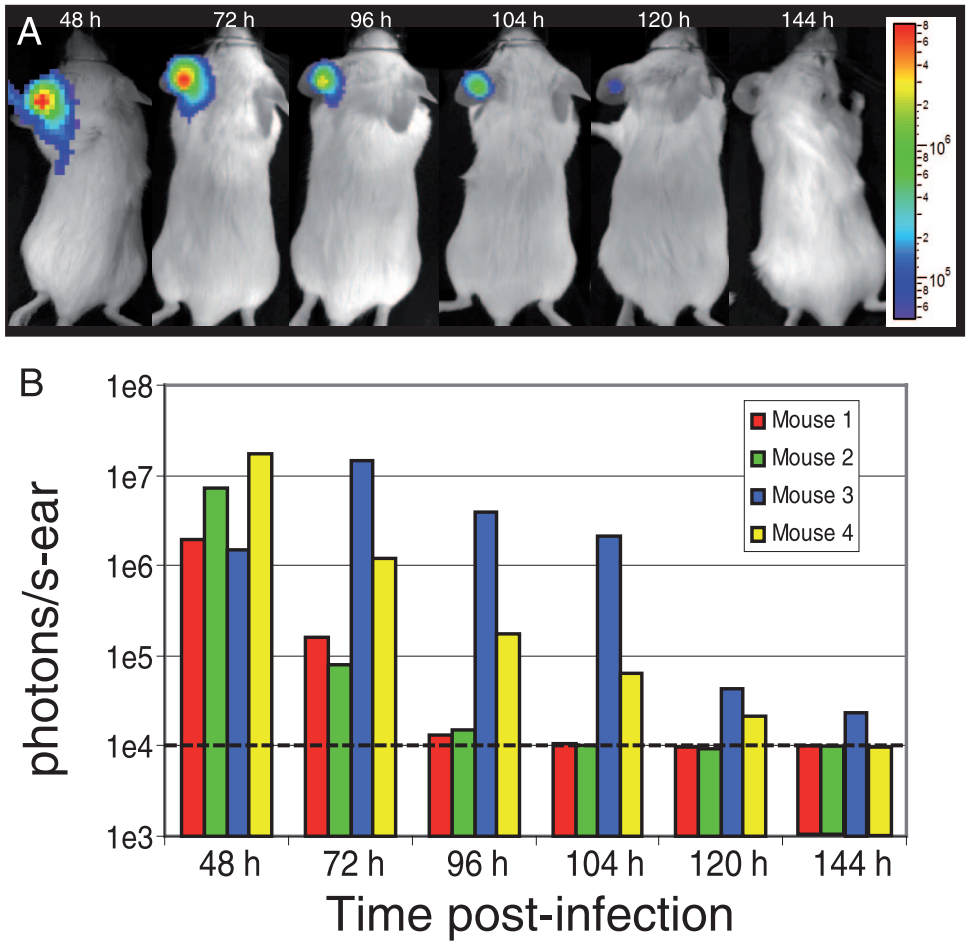

FIG. 3. BALB/c mice resist and eventually eliminate Tox$^+$ *B. anthracis* from cutaneous infections. (A) 9602Rlux spores (2×10^6) were injected into the ears of BALB/c mice and then analyzed as described in the legend to Fig. 1. Dorsal images of a single mouse are shown. The image series is representative of 12 infected mice. (B) The luminescence of the ears of mice was quantified at the indicated times by defining specific ROI encompassing the ear. Four individual mice are represented in the graph as differently colored bars. The dotted line represents the detection limit of luminescence.

infection in control mice than that in actively infected PA-immunized mice ($P = 0.033$; $n = 7$) (Fig. 4C). Luminescence in the ears of control mice intensified until death (Fig. 4C) and spread to deeper tissues, similar to the case for naïve mice described above (Fig. 1 and data not shown). One exceptional control mouse (number 4) showed no luminescence until 80 h postinfection, which then became a fulminant infection that killed the mouse, reminiscent of human and primate diseases that occurred long after exposure to spores (1, 20). These data imply that PA immunization limits bacterial growth to the cutaneous site of injection, without detectable bacterial growth in lymphoid tissues, and reduces bacterial growth from the earliest stages of infection.

DISCUSSION

Analysis of Tox$^+$ *B. anthracis* infections in mice revealed important differences in the progression of infection from that of previously reported Cap$^+$ bacteria (16). The Tox$^+$ strain (9602Rlux) remained confined to the ear longer than the Cap$^+$ strain, progressed to the draining lymph node, and finally was found in the lungs, kidneys, and defined points in the intestines and the pyloric region of the stomach. The most striking difference was observed in the spleen; at no point were there great numbers of bacteria found in this organ, as measured by either luminescence or CFU. In contrast, within 24 h Cap$^+$ bacteria spread from the ear to the draining lymph node, and by 36 h, they became detectable in the spleen before progressing to the lungs and blood, with minimal involvement of other organs until septicemia (16). It is unclear why such a marked difference exists in the spleen, but one might hypothesize that the spleen, an organ composed of a diverse collection of immune cells, can more efficiently resist infection by noncapsulated strains than by capsulated strains. Indeed, the capsule has been shown to reduce phagocytosis (25), while eliminating *B. anthracis* toxin production does not affect the virulence of capsulated strains in mice (6, 45). This suggests that, because of their lack of capsule and despite the production of toxins, Tox$^+$ 9602Rlux bacteria may be controlled in the spleen through phagocytosis-dependent mechanisms. Phagocytosis could both limit bacterial access to nutrients (2) and expose bacteria to toxic defense mechanisms (21), thereby reducing bacterial growth and luminescence and potentially leading to bacterial death.

Toxin production by Tox$^+$ bacteria may also influence dis-

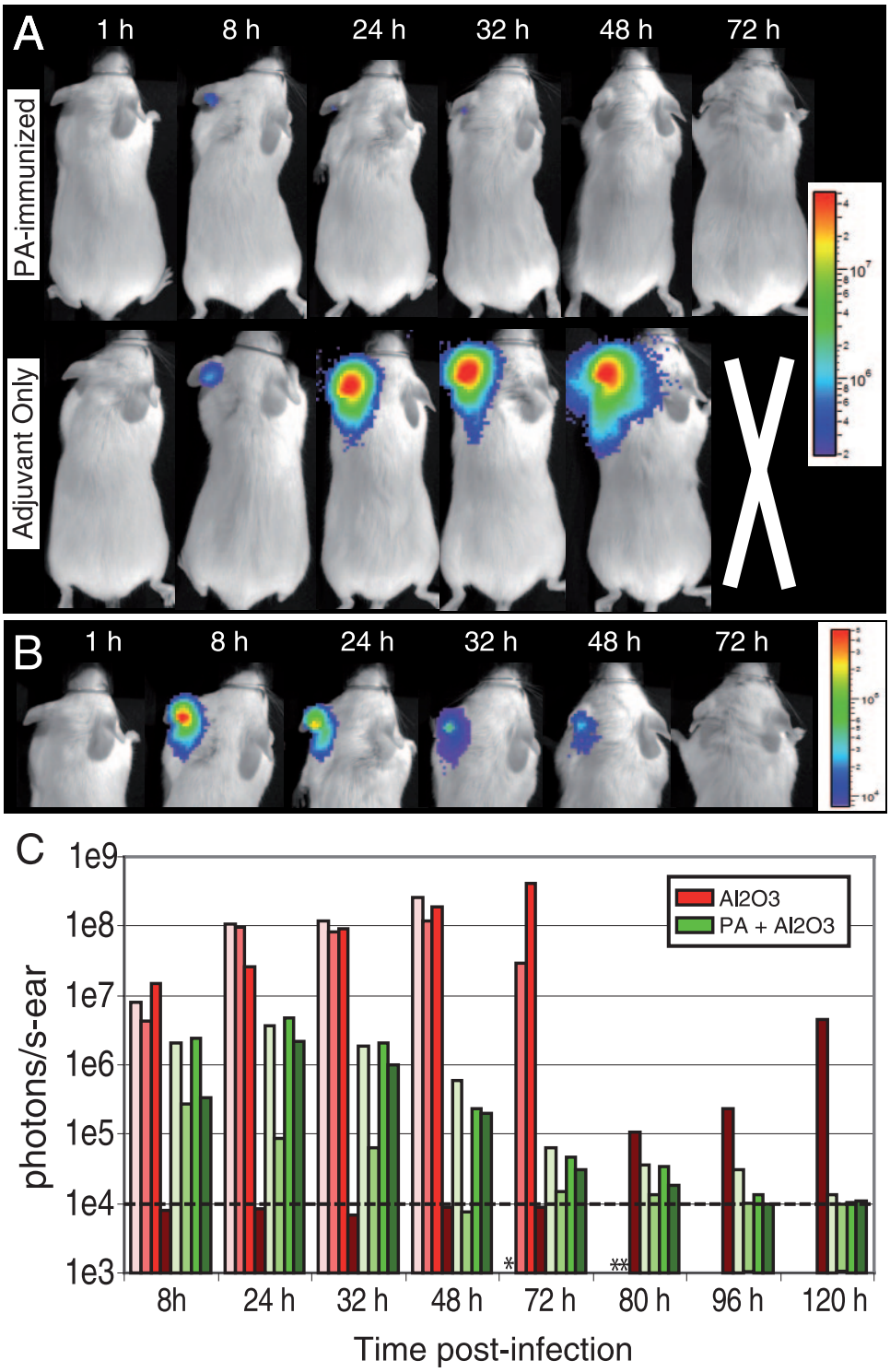

FIG. 4. Tox+ spores germinate in PA-immunized A/J mice but are confined to the site of inoculation. (A) PA-immunized (top) or adjuvant-only control (bottom) A/J mice were injected with 2×10^5 9602Rlux spores in the ear and then analyzed as described in the legend to Fig. 1. Dorsal views of a single representative PA-immunized and a single control mouse are shown, using the same scale. Each series is representative of eight immune or eight control mice. (B) Dorsal images of the head of the same PA-immunized mouse as that shown in panel A, using a lower luminescence scale. (C) Luminescence was quantified for the ears of PA-immune (PA + Al2O3; green bars) and adjuvant-only control (Al2O3; red bars) mice at the indicated times by defining specific ROI encompassing the ear. The dotted line represents the detection limit of luminescence. *, the corresponding control mouse died. No PA-immune mice died.

semination. Both LT and ET can cause cell death (10, 28) and thus can compromise endothelial barriers to the blood system. Indeed, hemorrhaging is often associated with anthrax (1). We suggest a model where Tox^+ bacteria begin growth at the site of inoculation and immediately begin secreting toxins. The toxins inhibit the protective inflammatory response and phagocyte chemotaxis (31) (which is further reduced in the C5-deficient sensitive mice) and thereby establish a relatively protected niche for multiplication. Bacteria continue to multiply and secrete toxins, as evident through clinical edema, eventually breaking down the barrier to the blood and giving bacteria access to the circulatory system. Additionally, once reaching and colonizing the draining lymph node, the Tox^+ bacteria could exit through the efferent lymphatics to the blood, as has been observed with fully virulent strains (24, 30). Upon gaining access to the blood, bacteria quickly traffic hematogenously and are trapped in the lungs, which are the first fine capillary bed encountered upon the return of blood from the periphery, and kidneys, whose major function is to filter blood. In these dissemination models, bacteria would also disseminate to the spleen, but as noted above, the spleen contains a large endogenous population of immune cells that may be able to limit the growth of the newly arrived uncapsulated bacteria.

An alternative, but not exclusive, hypothesis to explain the differences in dissemination of Tox^+ bacteria versus Cap^+ bacteria is based on a model of host cell-dependent transport. Bacteria have been observed in both the spore and replicative vegetative forms within phagocytes (32). Additionally, other studies have proposed that *B. anthracis* can be transported across epithelial barriers by macrophage chemotaxis to lymphoid organs (17, 30). However, LT has also been shown to efficiently kill some macrophages (28), so Tox^+ strains would rapidly kill the cells in which they are being transported, thus releasing bacteria into the blood to disseminate as free bacteria, similar to the scenario described above. Such a process would not occur for the Cap^+ strains, since they do not produce toxins. Instead, nascent Cap^+ bacteria would be predicted not to immediately kill the host cell, thus allowing transport within the phagocyte. Based on previously published observations (16), the initial chemotactic destination of the phagocyte would be predicted to be the draining lymph node, followed later by the spleen.

Tox^+ 9602Rlux cutaneous infections frequently disseminated to the gastrointestinal tract and kidneys, whereas Cap^+ bacteria did not (16). Furthermore, we observed the accumulation of liquid within the intestines, as previously observed through intravenous injection of purified ET (10), suggesting that the gastrointestinal tract is intoxicated by Tox^+ bacteria. Although gastrointestinal anthrax is connected with the consumption of contaminated food (3), colonization of the digestive tract is also linked to hematogenous spread of *B. anthracis*, which can occur in both inhalational and cutaneous infections (1). Thus, it remains unclear whether toxin activity prepares the gastrointestinal tract for colonization or whether bacteria first associate with the gastrointestinal tract, leading to localized targeting of toxins by implanted bacteria.

Immunization with PA is an effective method of preventing anthrax (42). Because anti-PA antibodies are protective and capable of neutralizing *B. anthracis* toxins (29), the humoral immune response is considered to be the primary effector of PA-based antianthrax immunity (23). In this study, we found that mice immunized with PA restricted Tox^+ 9602Rlux growth to the site of infection within the ear and prevented bacterial growth in other tissues, implying that immunity is immediately functional in situ. This observation supports the conclusion that preformed effectors, such as antibodies or PA-reactive CD4 T lymphocytes (22), act to restrict early bacterial growth. Anti-PA antibodies may neutralize the secreted toxins, opsonize spores to increase killing, and/or inhibit germination (40, 41). Concomitantly, CD4 T lymphocytes could augment the inflammatory response (14), allowing more efficient clearance of bacteria. Indeed, significantly less luminescence was observed in the ears of PA-immunized mice from the earliest times postinfection. This observation supports but does not differentiate between the role of antibodies in reducing the germination rate of spores in vivo, as previously shown in vitro (41), and their role in augmenting bacterial clearance by phagocytes (40).

Although toxinogenic noncapsulated strains of *B. anthracis* have been used to model infection, one of their original uses was as live vaccine strains (27). Indeed, these vaccines, administered by inoculation as live Tox^+ spores, are considered more effective than cell-free vaccines at establishing protective immunity (42), yet the inherent risk of live vaccines has deemed them inappropriate for human use (27). Accordingly, using BLI, we found that resistant BALB/c mice developed robust infections that lasted several days upon infection with Tox^+ spores, but the mice eventually controlled and cleared the infections. Through this multiday process, the adaptive immune system can become sufficiently activated by the presence of multiplying bacteria (15), toxin secretion, and a wide range of antigens to establish a highly effective protective immunity, perhaps explaining why these live vaccines are more efficacious than cell-free vaccines.

Infections of A/J and DBA/2 mice with Tox^+ *B. anthracis* strains, such as the Sterne strain, have been developed as models for anthrax because these mouse strains are particularly sensitive to *B. anthracis* infection. A/J and DBA/2 mouse sensitivities have been correlated with their inability to produce functional C5 (19, 43). However, the lack of C5 increases susceptibility only to noncapsulated bacterial strains (43), suggesting that capsulation renders C5 ineffective at impeding infection. This brought into question whether the differences in the locations of disseminated bacteria between the Tox^+ 9602Rlux strain, observed in this study in sensitive mice, and a Cap^+ strain in resistant mice reflect differences in mouse defenses or the presence or absence of toxins or capsule. However, we found that Cap^+ bacteria localized identically in both resistant BALB/c and sensitive A/J mice (data not shown), suggesting that bacterial localization characteristics are dependent on bacterial factors, not the mouse strain.

Real-time in vivo detection of bioluminescent *B. anthracis* spread has allowed the detection of previously unidentified differences between a toxin-producing noncapsulated strain (Tox^+) and a nontoxinogenic capsulated strain (Cap^+). Considering these differences, our data suggest that when using attenuated strains to model anthrax, each model must be matched with the specific question being asked, i.e., Tox^+ strains are appropriate for dissecting effects on the host caused by toxin secretion, whereas Cap^+ strains are better suited for

the examination of bacterial growth and dissemination. Whether a fully virulent Tox+ Cap+ strain will display dissemination characteristics reflecting a combination of those of the individual Tox+ and Cap+ strains or whether the combined virulence factors will synergize to yield a completely different pattern of infection remains to be determined.

ACKNOWLEDGMENTS

We thank Marie-Anne Nicola at the Plate-Forme d'Imagerie Dynamique at the Pasteur Institute for her valuable and consistent aid with bioluminescence imaging.

This study was supported in part by the Judith P. Sulzberger Postdoctoral Fellowship from The Pasteur Foundation of New York (I.J.G.), the CNRS, and the Institut Pasteur. The authors have no competing financial interests with this study.

REFERENCES

1. **Abramova, F. A., L. M. Grinberg, O. V. Yampolskaya, and D. H. Walker.** 1993. Pathology of inhalational anthrax in 42 cases from the Sverdlovsk outbreak of 1979. Proc. Natl. Acad. Sci. USA **90:**2291–2294.
2. **Appelberg, R.** 2006. Macrophage nutriprive antimicrobial mechanisms. J. Leukoc. Biol. **79:**1117–1128.
3. **Beatty, M. E., D. A. Ashford, P. M. Griffin, R. V. Tauxe, and J. Sobel.** 2003. Gastrointestinal anthrax: review of the literature. Arch. Intern. Med. **163:** 2527–2531.
4. **Belkaid, Y., S. Mendez, R. Lira, N. Kadambi, G. Milon, and D. Sacks.** 2000. A natural model of *Leishmania major* infection reveals a prolonged "silent" phase of parasite amplification in the skin before the onset of lesion formation and immunity. J. Immunol. **165:**969–977.
5. **Berthier, M., J. L. Fauchere, and J. Perrin.** 1996. Fulminant meningitis due to *Bacillus anthracis* in 11-year-old girl during Ramadan. Lancet **347:**828.
6. **Brossier, F., M. Levy, and M. Mock.** 2002. Anthrax spores make an essential contribution to vaccine efficacy. Infect. Immun. **70:**661–664.
7. **Candela, T., and A. Fouet.** 2005. *Bacillus anthracis* CapD, belonging to the gamma-glutamyltranspeptidase family, is required for the covalent anchoring of capsule to peptidoglycan. Mol. Microbiol. **57:**717–726.
8. **Collier, R. J., and J. A. Young.** 2003. Anthrax toxin. Annu. Rev. Cell Dev. Biol. **19:**45–70.
9. **Drysdale, M., S. Heninger, J. Hutt, Y. Chen, C. R. Lyons, and T. M. Koehler.** 2004. Capsule synthesis by *Bacillus anthracis* is required for dissemination in murine inhalation anthrax. EMBO J. **24:**221–227.
10. **Firoved, A. M., G. F. Miller, M. Moayeri, R. Kakkar, Y. Shen, J. F. Wiggins, E. M. McNally, W. J. Tang, and S. H. Leppla.** 2005. *Bacillus anthracis* edema toxin causes extensive tissue lesions and rapid lethality in mice. Am. J. Pathol. **167:**1309–1320.
11. **Francis, K. P., D. Joh, C. Bellinger-Kawahara, M. J. Hawkinson, T. F. Purchio, and P. R. Contag.** 2000. Monitoring bioluminescent *Staphylococcus aureus* infections in living mice using a novel *luxABCDE* construct. Infect. Immun. **68:**3594–3600.
12. **Friedlander, A. M.** 1997. Anthrax, p. 467–478. *In* F. R. Sidell et al. (ed.), Medical aspects of chemical and biological warfare. Office of The Surgeon General, Borden Institute, Walter Reed Army Medical Center, Washington, DC.
13. **Fukao, T.** 2004. Immune system paralysis by anthrax lethal toxin: the roles of innate and adaptive immunity. Lancet Infect. Dis. **4:**166–170.
14. **Glomski, I. J., J. P. Corre, M. Mock, and P. L. Goossens.** 2007. Cutting edge: IFN-{gamma}-producing CD4 T lymphocytes mediate spore-induced immunity to capsulated *Bacillus anthracis*. J. Immunol. **178:**2646–2650.
15. **Glomski, I. J., J. H. Fritz, S. J. Keppler, V. Balloy, M. Chignard, M. Mock, and P. L. Goossens.** 2007. Murine splenocytes produce inflammatory cytokines in a MyD88-dependent response to *Bacillus anthracis* spores. Cell. Microbiol. **9:**502–513.
16. **Glomski, I. J., A. Piris-Gimenez, M. Huerre, M. Mock, and P. L. Goossens.** 2007. Primary involvement of pharynx and Peyer's patch in inhalational and intestinal anthrax. PLoS Pathog. **3:**e76.
17. **Guidi-Rontani, C.** 2002. The alveolar macrophage: the Trojan horse of *Bacillus anthracis*. Trends Microbiol. **10:**405–409.
18. **Hardy, J., K. P. Francis, M. DeBoer, P. Chu, K. Gibbs, and C. H. Contag.** 2004. Extracellular replication of *Listeria monocytogenes* in the murine gall bladder. Science **303:**851–853.
19. **Harvill, E. T., G. Lee, V. K. Grippe, and T. J. Merkel.** 2005. Complement depletion renders C57BL/6 mice sensitive to the *Bacillus anthracis* Sterne strain. Infect. Immun. **73:**4420–4422.
20. **Henderson, D. W., S. Peacock, and F. C. Belton.** 1956. Observations on the prophylaxis of experimental pulmonary anthrax in the monkey. J. Hyg. (London) **54:**28–36.
21. **Kang, T. J., M. J. Fenton, M. A. Weiner, S. Hibbs, S. Basu, L. Baillie, and A. S. Cross.** 2005. Murine macrophages kill the vegetative form of *Bacillus anthracis*. Infect. Immun. **73:**7495–7501.
22. **Laughlin, E. M., J. D. Miller, E. James, D. Fillos, C. C. Ibegbu, R. S. Mittler, R. Akondy, W. Kwok, R. Ahmed, and G. Nepom.** 2007. Antigen-specific CD4+ T cells recognize epitopes of protective antigen following vaccination with an anthrax vaccine. Infect. Immun. **75:**1852–1860.
23. **Leppla, S. H., J. B. Robbins, R. Schneerson, and J. Shiloach.** 2002. Development of an improved vaccine for anthrax. J. Clin. Investig. **110:**141–144.
24. **Lincoln, R. E., D. R. Hodges, F. Klein, B. G. Mahlandt, W. I. Jones, Jr., B. W. Haines, M. A. Rhian, and J. S. Walker.** 1965. Role of the lymphatics in the pathogenesis of anthrax. J. Infect. Dis. **115:**481–494.
25. **Makino, S., I. Uchida, N. Terakado, C. Sasakawa, and M. Yoshikawa.** 1989. Molecular characterization and protein analysis of the cap region, which is essential for encapsulation in *Bacillus anthracis*. J. Bacteriol. **171:**722–730.
26. **Moayeri, M., and S. H. Leppla.** 2004. The roles of anthrax toxin in pathogenesis. Curr. Opin. Microbiol. **7:**19–24.
27. **Mock, M., and A. Fouet.** 2001. Anthrax. Annu. Rev. Microbiol. **55:**647–671.
28. **Park, J. M., F. R. Greten, Z. W. Li, and M. Karin.** 2002. Macrophage apoptosis by anthrax lethal factor through p38 MAP kinase inhibition. Science **297:**2048–2051.
29. **Pitt, M. L., S. Little, B. E. Ivins, P. Fellows, J. Boles, J. Barth, J. Hewetson, and A. M. Friedlander.** 1999. In vitro correlate of immunity in an animal model of inhalational anthrax. J. Appl. Microbiol. **87:**304.
30. **Ross, J. M.** 1957. The pathogenesis of anthrax following the administration of spores by the respiratory route. J. Pathol. Bacteriol. **73:**485–494.
31. **Rossi Paccani, S., F. Tonello, L. Patrussi, N. Capitani, M. Simonato, C. Montecucco, and C. T. Baldari.** 2007. Anthrax toxins inhibit immune cell chemotaxis by perturbing chemokine receptor signalling. Cell. Microbiol. **9:**924–929.
32. **Ruthel, G., W. J. Ribot, S. Bavari, and T. A. Hoover.** 2004. Time-lapse confocal imaging of development of *Bacillus anthracis* in macrophages. J. Infect. Dis. **189:**1313–1316.
33. **Schneerson, R., J. Kubler-Kielb, T. Y. Liu, Z. D. Dai, S. H. Leppla, A. Yergey, P. Backlund, J. Shiloach, F. Majadly, and J. B. Robbins.** 2003. Poly(gamma-D-glutamic acid) protein conjugates induce IgG antibodies in mice to the capsule of *Bacillus anthracis*: a potential addition to the anthrax vaccine. Proc. Natl. Acad. Sci. USA **100:**8945–8950.
34. **Spencer, R. C.** 2003. *Bacillus anthracis*. J. Clin. Pathol. **56:**182–187.
35. **Sylvestre, P., E. Couture-Tosi, and M. Mock.** 2005. Contribution of ExsFA and ExsFB proteins to the localization of BclA on the spore surface and to the stability of the *Bacillus anthracis* exosporium. J. Bacteriol. **187:**5122–5128.
36. **Sylvestre, P., E. Couture-Tosi, and M. Mock.** 2003. Polymorphism in the collagen-like region of the *Bacillus anthracis* BclA protein leads to variation in exosporium filament length. J. Bacteriol. **185:**1555–1563.
37. **Tournier, J. N., A. Quesnel-Hellmann, A. Cleret, and D. R. Vidal.** 2007. Contribution of toxins to the pathogenesis of inhalational anthrax. Cell. Microbiol. **9:**555–565.
38. **Tournier, J. N., A. Quesnel-Hellmann, J. Mathieu, C. Montecucco, W. J. Tang, M. Mock, D. R. Vidal, and P. L. Goossens.** 2005. Anthrax edema toxin cooperates with lethal toxin to impair cytokine secretion during infection of dendritic cells. J. Immunol. **174:**4934–4941.
39. **Van den Broeck, W., A. Derore, and P. Simoens.** 2006. Anatomy and nomenclature of murine lymph nodes: descriptive study and nomenclatory standardization in BALB/cAnNCrl mice. J. Immunol. Methods **312:**12–19.
40. **Welkos, S., A. Friedlander, S. Weeks, S. Little, and I. Mendelson.** 2002. In-vitro characterisation of the phagocytosis and fate of anthrax spores in macrophages and the effects of anti-PA antibody. J. Med. Microbiol. **51:**821–831.
41. **Welkos, S., S. Little, A. Friedlander, D. Fritz, and P. Fellows.** 2001. The role of antibodies to *Bacillus anthracis* and anthrax toxin components in inhibiting the early stages of infection by anthrax spores. Microbiology **147:**1677–1685.
42. **Welkos, S. L., and A. M. Friedlander.** 1988. Comparative safety and efficacy against *Bacillus anthracis* of protective antigen and live vaccines in mice. Microb. Pathog. **5:**127–139.
43. **Welkos, S. L., and A. M. Friedlander.** 1988. Pathogenesis and genetic control of resistance to the Sterne strain of *Bacillus anthracis*. Microb. Pathog. **4:**53–69.
44. **Welkos, S. L., T. J. Keener, and P. H. Gibbs.** 1986. Differences in susceptibility of inbred mice to *Bacillus anthracis*. Infect. Immun. **51:**795–800.
45. **Welkos, S. L., N. J. Vietri, and P. H. Gibbs.** 1993. Nontoxigenic derivatives of the Ames strain of *Bacillus anthracis* are fully virulent for mice: role of plasmid pX02 and chromosome in strain-dependent virulence. Microb. Pathog. **14:**381–388.

Editor: V. J. DiRita